Clinical & Experimental Metastasis **20:** 451–458, 2003.

Continuous real time *ex vivo* epifluorescent video microscopy for the study of metastatic cancer cell interactions with microvascular endothelium

Olga V. Glinskii[2,4], Virginia H. Huxley[2,3], James R. Turk[3], Susan L. Deutscher[1,4], Thomas P. Quinn[1], Kenneth J. Pienta[5,6] & Vladislav V. Glinsky[1,4]

Departments of [1]Biochemistry, [2]Physiology, and [3]Veterinary Biomedical Sciences, University of Missouri, Columbia, Missouri, USA; [4]Harry S. Truman Memorial Veterans Hospital, Columbia, Missouri, USA; Departments of [5]Internal Medicine and [6]Urology, University of Michigan, Ann Arbor, Michigan, USA

Received 9 December 2002; accepted in revised form 27 January 2003

Key words: adhesion, dura mater, intravascular, metastasis, porcine, prostate carcinoma, video microscopy

Abstract

Recent studies suggest that only endothelium-attached malignant cells are capable of giving rise to hematogenous cancer metastases. Moreover, tumor cell adhesion to microvascular endothelium could be crucial in metastasis predilection to specific organs or tissues. However, the existing *in vitro* and *in vivo* techniques do not provide for sufficient delineation of distinct stages of a dynamic multi-step intravascular adhesion process. Here we report the development of an experimental system allowing for prolonged continuous *ex vivo* real-time observation of malignant cell adhesive interactions with perfused microvessels of a target organ in the context of its original tissue. Specifically, the vasculature of excised dura mater perfused with prostate cancer cells is described. An advantage of this technique is that selected fluorescently labeled tumor cells can be followed along identified vascular trees across the entire tissue specimen. The techniques provide for superior microvessel visualization and allow for uninterrupted monitoring and video recording of subsequent adhesion events such as rolling, docking (initial reversible adhesion), locking (irreversible adhesion), and flattening of metastatic cancer cells within perfused microvasculature on a single cell level. The results of our experiments demonstrate that intravascular adhesion of cancer cells differs dramatically from such of the leukocytes. Within dura microvessels perfused at physiological rate, non-interacting, floating, tumor cells move at velocities averaging 7.2×10^3 μm/s. Some tumor cells, similarly to leukocytes, exhibit rolling-like motion patterns prior to engaging into more stable adhesive interactions. In contrast, other neoplastic cells became stably adhered without rolling showing a rapid reduction in velocity from 2×10^3 to 0 μm/s within fractions of a second. The experimental system described herein, while developed originally for studying prostate cancer cell interactions with porcine dura mater microvasculature, offers great flexibility in adhesion experiments design and is easily adapted for use with a variety of other tissues including human.

Introduction

Discovering the molecular mechanisms underpinning cancer metastasis is one of the most important goals of modern cancer research. After metastatic cancer cells escape the primary tumor and enter a circulation, interactions of blood borne malignant cells with microvascular endothelium represent the first and rate-limiting step in establishing of secondary metastatic lesions. Recently, it was shown that only endothelium-attached tumor cells are capable of giving rise to hematogenous metastases [1]. These results underscored the critical importance of tumor-endothelial cell interactions in metastatic cancer spread.

Many important facts regarding cancer cell adhesion to endothelia were revealed *in vitro*, using static adhesion assays and parallel flow chamber techniques, or *in vivo*, employing intravital video microscopy [2]. Yet, the existing *in vitro* and *in vivo* experimental approaches have numerous major limitations. Most importantly, they do not allow for a sufficient delineation of the specific functions of different adhesion molecules at distinct stages of cancer metastasis as well as for continuous monitoring of individual metastatic cell interactions with intact host microvessels in the context of its original tissue over a prolonged period of time. However, studying adhesion processes without loss of their original microenvironment and temporal dynamics is crucial for obtaining the most accurate and reliable information [3].

Current models of cancer cell adhesion to the microvasculature describe it as a multi-step process including priming (changes in the endothelium adhesiveness), docking (initial reversible cancer cell adhesion to the endothelium), locking (irreversible adhesion involving protein-protein interactions), followed by extravasation and/or intravascular clonogenic growth [1, 4, 5]. A broad array of adhesion

Correspondence to: Vladislav V. Glinsky, MD, M121 Medical Sciences Bldg, Department of Biochemistry, University of Missouri, Columbia, MO 65212, USA. Tel: +1-573-814-6000, ext. 3691; Fax: +1-573-814-6551; E-mail: glinskiivl@missouri.edu

molecules such as carbohydrates, lectins, cadherins, and integrins participate at distinct stages of this process, whereas the unique combination of the adhesion molecules expressed on tumor and endothelial cells may predetermine the outcome of both the adhesion and the metastatic process in whole. Indeed, a possible role for these interactions in defining tissue specificity of breast and prostate cancer metastasis was revealed [5–8]. For example, the preferential adhesion of prostate cancer cells to bone marrow derived endothelium was demonstrated [7], and two independent groups have shown that human prostate cancer cells exhibit striking tissue specificity in humanized animal models of cancer metastasis [9, 10]. These findings once again highlighted the necessity of studying malignant cell adhesive interactions with intact microvasculature of the specific organs and tissues.

Here we report the development of the experimental system allowing for a prolonged (up to several hours), continuous *ex vivo* real time observation of malignant cells adhesive interactions with perfused porcine microvessels. The use of porcine tissue provides for studying cancer-endothelial cell interactions with intact differentiated microvessels of a large mammalian species exhibiting considerable well-characterized similarities in microvascular physiology and cellular biochemistry with humans [11]. Specifically, in this study, we used dura mater, a tissue representing an important site of intracranial malignant involvements targeted frequently by prostate cancer metastasis (Figure 1A). Although, until lately, the incidence of dura mater metastases has been underreported, in a recent autopsy series of men who died from advanced hormone-refractory prostate cancer, metastatic tumors originated from dura mater were found in 43% of the cases [12].

Our experiments demonstrated that intravascular cancer cell adhesion behavior differs dramatically from that of leukocytes. Within dura mater microvasculature perfused at physiological rate, non-interacting tumor cells moved at high velocities averaging 7.19×10^3 μm/s. Whereas some tumor cells, similarly to leukocytes, exhibited rolling-like motion patterns prior to engaging into more stable adhesive interactions; other became stably adhered without rolling, showing a rapid reduction in velocity from 2×10^3 to 0 μm/s within fractions of a second. It is well documented that leukocytes adhere to the endothelia and escape microcirculation in post capillary venules. In contrast, even though we cannot completely rule out cancer cell adhesion to venular endothelium, we observed the prevailing majority of neoplastic-endothelial cell adhesion in pre capillary arterioles and capillaries. Moreover, even within the arterial part of a vascular tree, tumor cell interactions with different microvessels varied significantly. Further, neoplastic cell adhesion behavior changes dynamically as they pass through different segments of the same blood vessel.

In summary, our results demonstrate fundamental differences in intravascular adhesion behavior between metastatic cancer cells and leukocytes suggesting that they could be driven by distinct molecular mechanisms. The non-uniform character of tumor cell adhesive interactions with different microvessels highlights the importance of studying in greater detail the role of the microvascular endothelium adhesive properties in hematogenous cancer spread.

Materials and methods

Chemicals and reagents

Sylgard® was purchased from Dow Corning Corp. (Midland, Michigan, USA). Oregon Green™-514 was obtained from Molecular Probes Inc. (Eugene, Oregon, USA). All other reagents, including porcine serum albumin, were purchased from Sigma Chemicals Co. (St. Louis, Missouri, USA), unless otherwise specified.

Tissue acquisition and preparation

The dura mater tissue was acquired from 9–12 month-old mature male Yucatan miniature swine undergoing cardiology procedure in the course of an unrelated study. Dura mater corresponding to one hemisphere (Figure 1B) was collected within 15–30 min after animal's sacrifice, and placed immediately on ice in a porcine Krebs solution (Krebs physiological salt supplemented with 1.0 mg/ml porcine albumin). Special attention was paid to minimize dura mater damage during its separation from the skull. The collected dura was rinsed twice with ice-cold porcine Krebs solution, and transferred to a refrigerated tissue dissection dish filled with porcine Krebs solution and connected to a circulating bath to maintain the sample temperature from 0 to 4 °C during the dissection procedure.

In our experiments, the collected dura mater corresponding to one hemisphere (Figure 1B) was dissected and trimmed under control of a low-power stereomicroscope SMZ-2B (Nikon, Japan) to remove arachnoid granulations and release dura's folds as to allow for a flattening tissue sample onto Sylgard-coated 100-mm tissue culture dish (Figure 1C). During the trimming, particular care was taken not to damage major blood vessels detectable under stereomicroscope. After choosing a point for cannulation on one of the branches of a median meningeal artery (Figure 1C), a 2–3 mm incision in a top layer of dura was made, and approximately 5 mm long segment of the artery was separated carefully from surrounding tissues. After that, the sample was transferred onto the fluorescent microscope stage, and the artery was cannulated using a pipette manufactured from 1 mm O.D. borosilicate glass capillary with 90 μm opening at the tip. From this point on, the experiments were performed at room temperature.

Human cancer cells

The DU-145 human prostate carcinoma cell line was obtained from the American Type Culture Collection (Rockville, Maryland, USA). The cells were maintained on plastic in a humidified incubator in 5% CO_2/95% air at 37 °C as a monolayer culture using RPMI-1640 medium supplemented with L-glutamine and 10% fetal bovine serum.

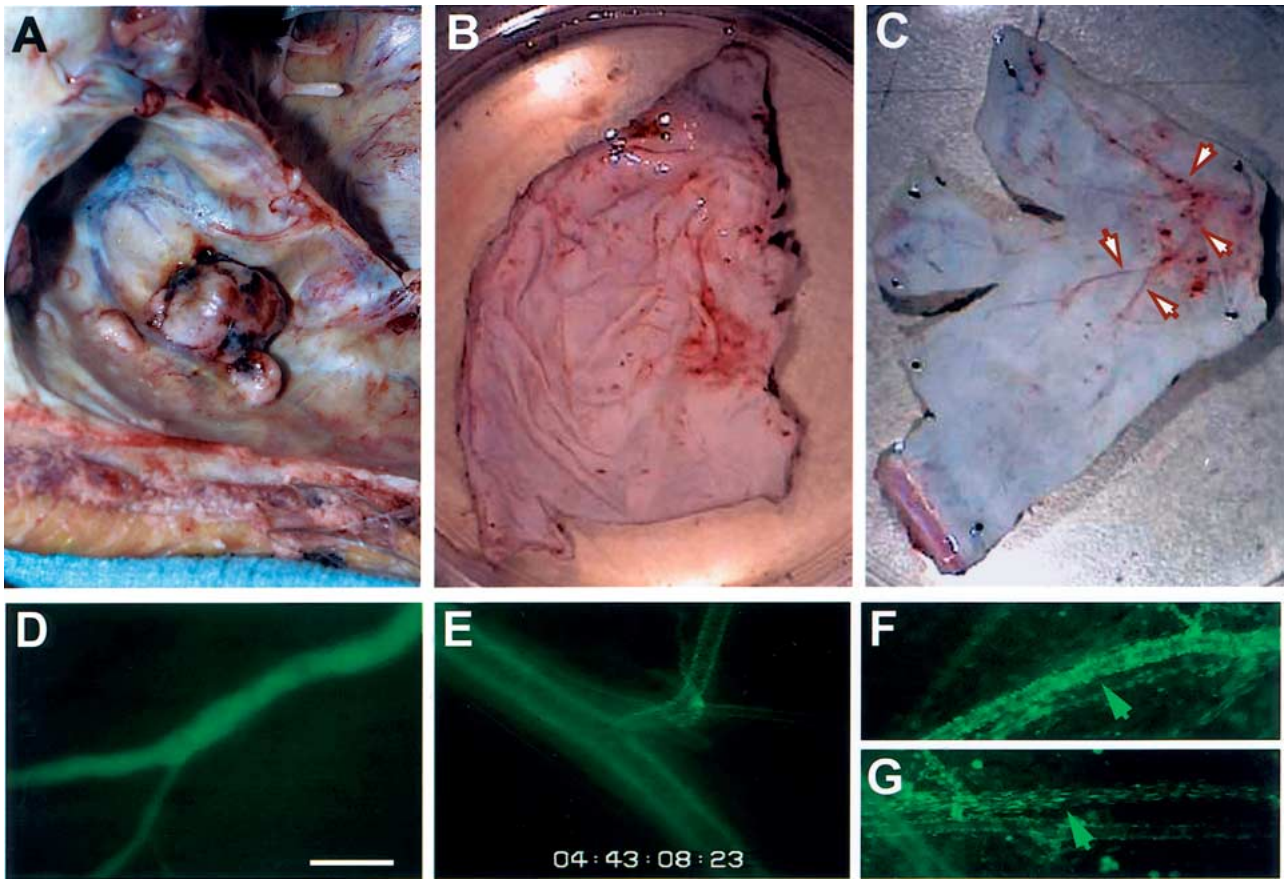

Figure 1. A, dura mater metastatic lesions of a hormone-refractory adenocarcinoma of the prostate. B and C, porcine dura mater corresponding to one hemisphere before (B) and after (C) dissecting and trimming to allow flattening on a Sylgard-coated tissue dish. Arrows indicate possible points for connecting to the branches of the median meningeal artery. D through G, dura mater microvessel contrasting using Oregon Green-labeled porcine albumin (D) and acridine orange (E–G). Acridine orange staining provides for permanent vessel contrasting leaving the vessel lumen free for observation of the adhesion events (E). Upon staining with acridine orange arteries (F) and veins (G) exhibit distinct staining patterns. Note presence of the smooth muscle nuclei oriented perpendicularly to the vessel axis on artery (F), whereas only endothelial cell nuclei oriented along the vessel axis could be seen on vein (G). Scale bar: 100 μm.

Immediately prior to adhesion experiments, cancer cells were prelabeled for 5 min with 3 μg/ml solution of acridine orange in RPMI-1640 medium, rinsed three times with serum free RPMI-1640 medium, dissociated from plastic using a nonenzymatic cell dissociation reagent (Sigma, St. Louis, Missouri, USA), and pipetted to produce a single cell suspension. To remove any remaining cell clumps, tumor cell suspension was filtered through a 20-μm nylon mesh, and adjusted to contain 5×10^4 cell/ml. A fresh neoplastic cell suspension was prepared prior to every injection.

Vessel perfusion and contrasting

After connecting to one of the branches of *Median Meningeal artery* (typically 300–500 μm I.D.), dura mater vasculature was perfused for 20 min with porcine Krebs solution using a precision syringe infusion/withdrawal pump KDS210 (KD Scientific, USA) at physiological rate (typically 15–30 μl/min). The physiological flow rate was estimated depending on vessel diameter based on literature data [13]. To visualize the perfused vascular tree, microvessels were perfused for additional 20–60 min either with porcine Krebs solution containing Oregon Green-514-labeled porcine albumin (1.0 mg/ml final albumin concentration), or with 0.3 μg/ml acridine orange solution in physiological porcine Krebs or RPMI-1640 media supplemented with 10% FBS and 1.0 mg/ml porcine albumin.

Video microscopy system

The video microscopy system was assembled on the basis of a fixed stage fluorescent microscope Laborlux 8 (Leitz Wetzlar, Germany), equipped with 75-watt Xenon illuminator and FITC and Rhodamine filter cubes. Video images were acquired with a high sensitivity monochrome solid-state CCD video camera (COHU Inc., San Diego, California, USA) and recorded using a Panasonic S-VHS videocassette recorder AG-MD830 (Panasonic, Japan) at 30 frames per second.

To enable the use of large tissue specimens, we designed an original experimental platform mounted directly on a fluorescent video microscope stage, capable of accommodating 100 mm dish and bearing a 'little giant' series three-dimensional micromanipulator (Narishige, Japan) coupled with an injector connected to the precision infusion pump. Introducing an inline low-pressure chromatography injector with all-teflon wetted parts (Rheodyne Model 50200, Rheodyne, USA), connected directly to the pipette, allows for

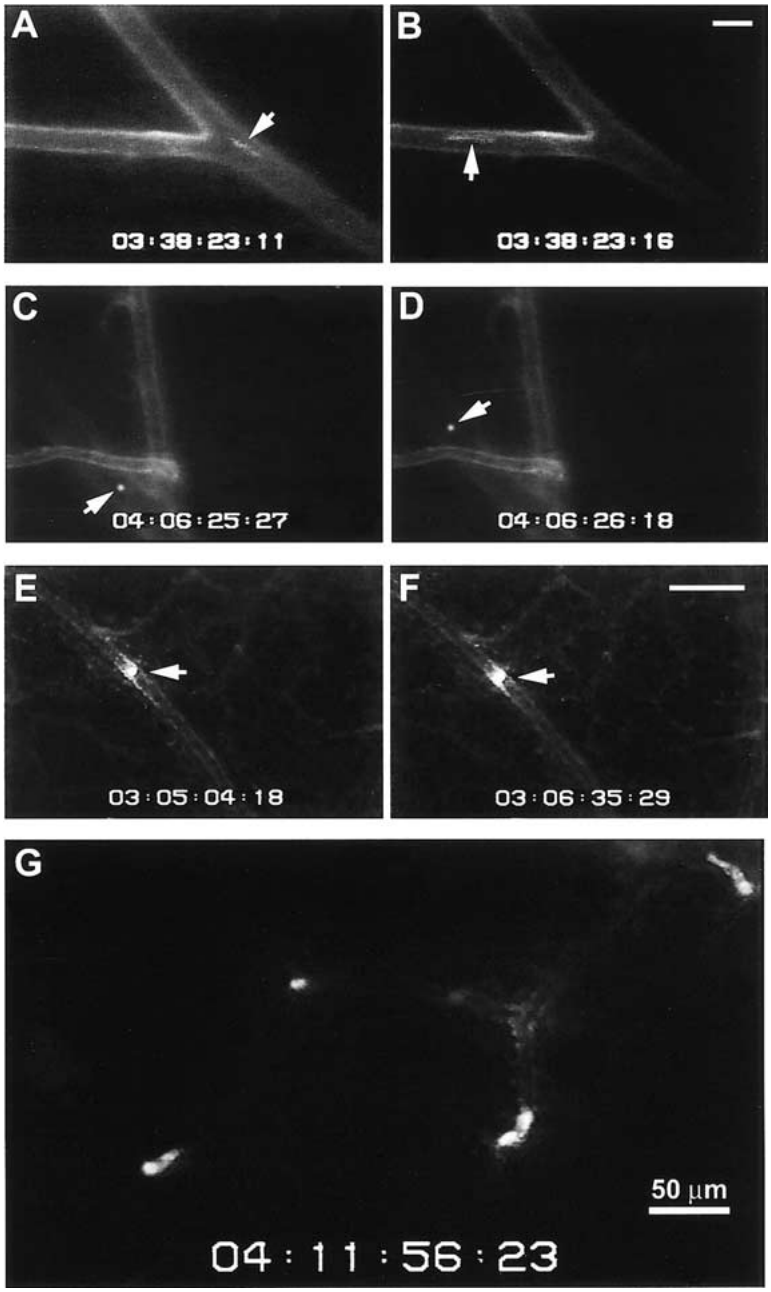

Figure 2. The appearance of non-interacting (A, B), interacting (rolling) (C, D), and stably adhered (E, F) cancer cells in a perfused porcine dura mater vasculature. Non-interacting (floating) cells at a physiological perfusion rate appear as a smear on a still frame. Two different floating cancer cells indicated by arrows, which passed through the same part of the vascular tree within 0.2 s from each other are shown in A and B. In contrast, interacting (rolling) cell moves significantly slower with frequent interruptions and stops (C, D). The difference between frames C and D is 0.7 s, during which tumor cell (arrows) covered the distance of approximately 70 μm. E and F, stably adhered cancer cell (arrows), which remains stationary in a microvasculature for a prolonged period of time. The difference between frames E and F is greater than 1.5 min. G, Stably adhered prostate cancer cells flattened within dura mater microvasculature after 4 h of perfusion. Scale bars: 50 μm; scale bar in B for frames A through D, scale bar in F for frames E and F.

injecting neoplastic cells in a precise volume, defined by a sample loop size, without interrupting perfusion. The platform allows for injecting a defined amount of fluorescently labeled tumor cells and monitoring their interactions with dura's microvasculature across the entire dura mater specimen corresponding to the whole hemisphere.

Image processing and data analysis

For subsequent frame-by frame analysis, the recorded analog video images were digitized using a media converter DVMC-DA2 (Sony, Japan) and Adobe Premier 6 software (Adobe Systems Inc., San Jose, California, USA). For better visual perception, the selected frames were pseudo colored using Adobe Photoshop 5.5 (Adobe Systems Inc., San Jose, California, USA) and MetaMorph Immaging System (Universal Imaging, Hallis, New Hampshire, USA) software.

Results and discussion

Blood vessel contrasting and visualization

The traditional approach to contrasting and visualizing a perfused microvasculature would be to inject one of the commonly used fluorophores such as FITC or fluorophore-tagged proteins such as Oregon Green- or Texas Red-labeled albumin [14]. The infusion of the fluorophore-labeled protein solution allows for sufficient visualization of a perfused vascular tree (Figure 1D), however, this technique only provides for transient microvessel contrast, which disappears as soon as the fluorophore is washed away. In addition, high background fluorescence of the vessel-contrasting compound interferes with the observation of intravascular adhesion events.

To overcome these limitations, we developed an original method for visualizing the microvasculature by perfusing it for 20–60 min (depending on a size of a perfused vascular tree) with a weak (0.3 μg/ml) acridine orange solution (Figure 1E). For our experiments, this technique provides several advantages over visualizing microvessels using fluorophore-labeled proteins. First, it results in a rapid and permanent staining of endothelial and smooth muscle cell nuclei allowing for viewing of perfused microvasculature in great detail. Importantly, photobleaching caused by prolonged illumination is insignificant, as even after 4 to 5 h the perfused vascular tree is clearly visible. Second, when focusing on a vessel surface, it allows for distinguishing between arteries and veins (Figures 1F and G) due to differences in staining patterns. The arteries, in addition to endothelial cell labeling, exhibit specific staining pattern due to the labeling of the oriented perpendicularly to the vessels axis nuclei of smooth muscle cells as well (Figure 1F). In contrast, only endothelial cell nuclei oriented strictly along the vessel axis could be seen on veins (Figure 1G). Third, the acridine orange staining to a certain extent allows for the monitoring of endothelial cells viability by periodically switching to higher magnification and checking on some of the early signs of apoptosis such as chromatin condensation or generation of single-stranded DNA specimens, which would result in shifting of green fluorescence of the acridine orange complexes with double-stranded DNA toward the red. Most importantly, this labeling technique leaves the vessel lumen free for observation of intravascular adhesion events. In addition, pre-perfusing dura mater vasculature prior to neoplastic cell injection, removes most blood elements from microcirculation thus eliminating their impact on the results of adhesion experiments.

Cancer cell injection, video microscopy, and subsequent analysis of cancer cell interactions with microvasculature

Metastatic cancer cells, including DU-145 human prostate carcinoma cells used in this study, posses enhanced homotypic aggregation ability [15]. Therefore, to prevent tumor cells from adhering to each other and forming multicellular clumps, it is important to prepare a single cell suspension of fluorescently labeled cancer cells immediately prior to injecting them. For same reason, it is highly desirable to minimize the time of cancer cell passage through the plastic tubes of the infusion system into the vasculature of the perfused tissue. To achieve this, we introduced a low-pressure chromatography injector with all-teflon vetted parts immediately next to the micromanipulator. This allowed us to connect the 'out' port of the injector directly to the pipette thus reducing the system 'dead' volume to approximately 80 μl. As a result, in our experiments, cancer cells appear in a perfused microvasculature within 3 min post injection. In addition, the inline injector allows for introduction of a precise amount of cancer cells in exactly the same volume defined by the size of a sample loop, as well as for multiple tumor cell injections at different time points without interrupting perfusion. In our experiments, we routinely use four to five 500 μl injections of cancer cell suspension with 30 min intervals between subsequent injections.

There are several options for monitoring and analyzing intravascular adhesion events. After injecting fluorescently labeled cancer cells, their adhesive interactions with microvasculature could be monitored and video recorded at a predetermined location within the vascular tree over a defined period of time. A subsequent frame-by-frame analysis is performed then to characterize the adhesion behavior of cancer cells, which passed through the observed microvessels. When perfused at the physiological flow rate, as measured in 90–100 μm in diameter arterioles, non-interacting (floating) tumor cells move at a high velocity averaging $7.19 \times 10^3 \pm 3.29 \times 10^3$ μm/s (range 1.6×10^3–16.5×10^3 μm/s with 72.2% in a range from 5.1×10^3 to 9.4×10^3 μm/s), and appear on a still frame as a smear (Figures 2A and B). Interestingly, at the beginning of the experiments, high tumor cell velocity is accompanied by a very low (3.3–3.7%) number of neoplastic cells interacting with endothelium. However, after 3 to 4 rounds of tumor cell injection (1.5–2 h of perfusion), the fraction of cancer cells actively interacting with microvessel walls increases to 24.3%. At this time, abundant prostate cancer cell interactions with dura mater microvessels, ranging from 110 μm to less than 20 μm in diameter, become available for observation. In contrast to non-interacting (floating) cells, tumor cells that interact with the vascular wall move at the velocities $\leq 2.0 \times 10^3$ μm/s. According to hydrodynamic studies, Poiseuille flow in blood vessels is characterized by a parabolic profile with highest velocities along the centerline, forcing larger free-floating particles, such as non-interacting leukocytes or cancer cells, to the center of the stream [16, 17]. Therefore, described herein reduction in tumor cell velocity reflects their displacement out of the center stream toward the blood vessel wall and is indicative of tumor cell interactions with microvascular endothelium. Upon circulating cell displacement toward the wall, both the shear force and specific adhesive interactions will regulate the rolling response [17]. For these reasons, we designated all tumor cells moving at velocity $\leq 2 \times 10^3$ μm/s as interacting/rolling cells. The interacting/rolling cells move significantly slower (Figures 2C and D). Some of the interacting/rolling cancer cells engage into more stable adhesive interactions and

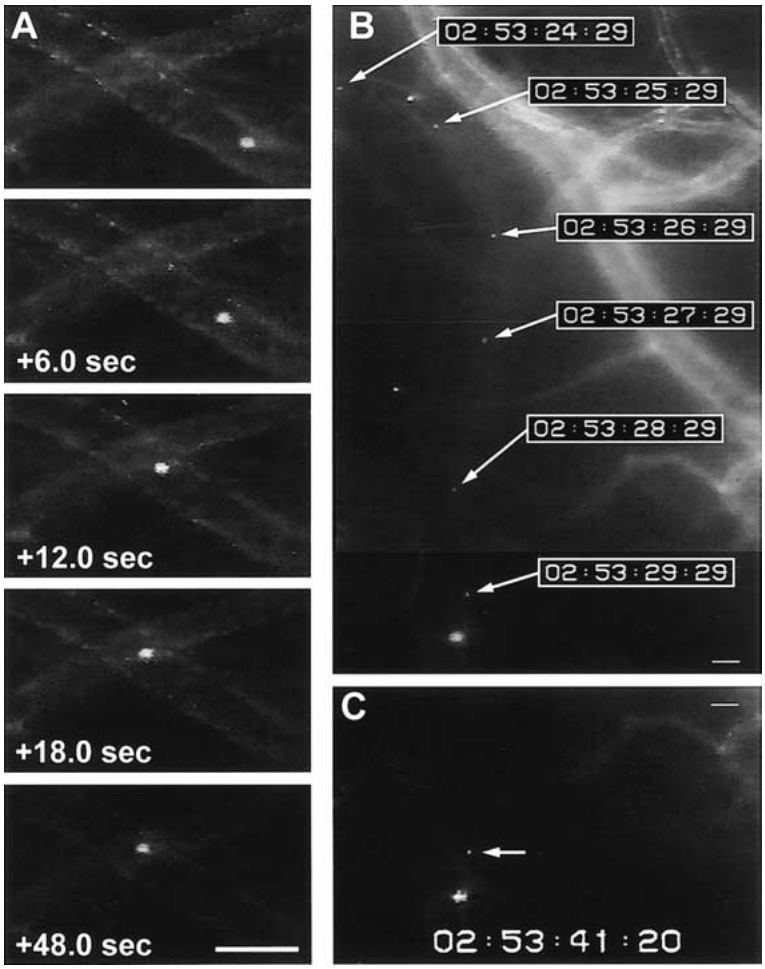

Figure 3. (A) Fluorescently labeled prostate carcinoma cell exhibiting, similarly to leukocytes, rolling-like movement prior to engaging into stable adhesive interactions. Time elapsed indicated at the bottom of each subsequent frame shown. Scale bar: 50 μm. (B and C) A composite image of 6 subsequent frames (B) showing fast moving neoplastic cell, which abruptly stops and becomes permanently adhered without rolling (B, C). Numbers in boxes show time code generator reading corresponding to each frame in hours, minutes, seconds, and frame numbers (30 frames/s) presented as hh:mm:ss:ff. Scale bar: 100 μm.

remain stationary for extended (>30 s) periods of time (Figures 2E and F), or become permanently attached to the vascular wall. In some cases, when permanent lodging occurs in microvessels of a size comparable with tumor cells (Figure 2G), it is hard to conclude whether neoplastic cell arrest was caused by a mechanical trapping or by specific adhesive interactions. On this basis, many have attributed tumor cell arrest in microcirculation entirely to mechanical mechanisms of size limitation. However, in many instances, we observed permanent tumor cell attachment to the vascular wall in microvessels far exceeding neoplastic cells in diameter (Figures 2E, 3A and 4C). In these cases, a mechanical factor could be clearly excluded, suggesting that specific adhesive interactions between malignant cells and endothelia mediate tumor cell arrest in the vasculature. The extension of a perfusion time up to 4–5 h enables for observing subsequent stages of the adhesion process resulting in malignant cells flattening on microvessels endothelia (Figure 2G). Alternatively, after tumor cell injection, selected individual neoplastic cells could be followed along the vasculature, and changes in their adhesion behavior observed and video recorded as they pass through different microcirculation compartments.

Tumor cell intravascular adhesion behavior differs from such of leukocytes

It is well documented that in leukocyte adhesion rolling is the first and rate-limiting step ultimately required for stable leukocyte adhesion to the endothelium [18]. In contrast, our results demonstrated that, whereas some malignant cells similarly to leukocytes exhibited rolling-like motion prior to engaging into more stable adhesive interactions (Figure 3A), other exhibited an adhesion behavior completely distinct from such of white blood cells. These neoplastic cells, moving at the velocity as high as 2×10^3 μm/sec, stopped momentarily and became attached to the vascular wall within fractions of a second (Figures 3B and C). Recently, we reported similar adhesion behavior of highly metastatic MDA-MB-435 human breast carcinoma cells *in vitro* in parallel flow chamber experiments [19]. Interestingly, while there was no difference between highly metastatic MDA-MB-435 and poorly metastatic MDA-MB-468 cells in their ability to roll on microvascular endothelium, the MDA-MB-435 were

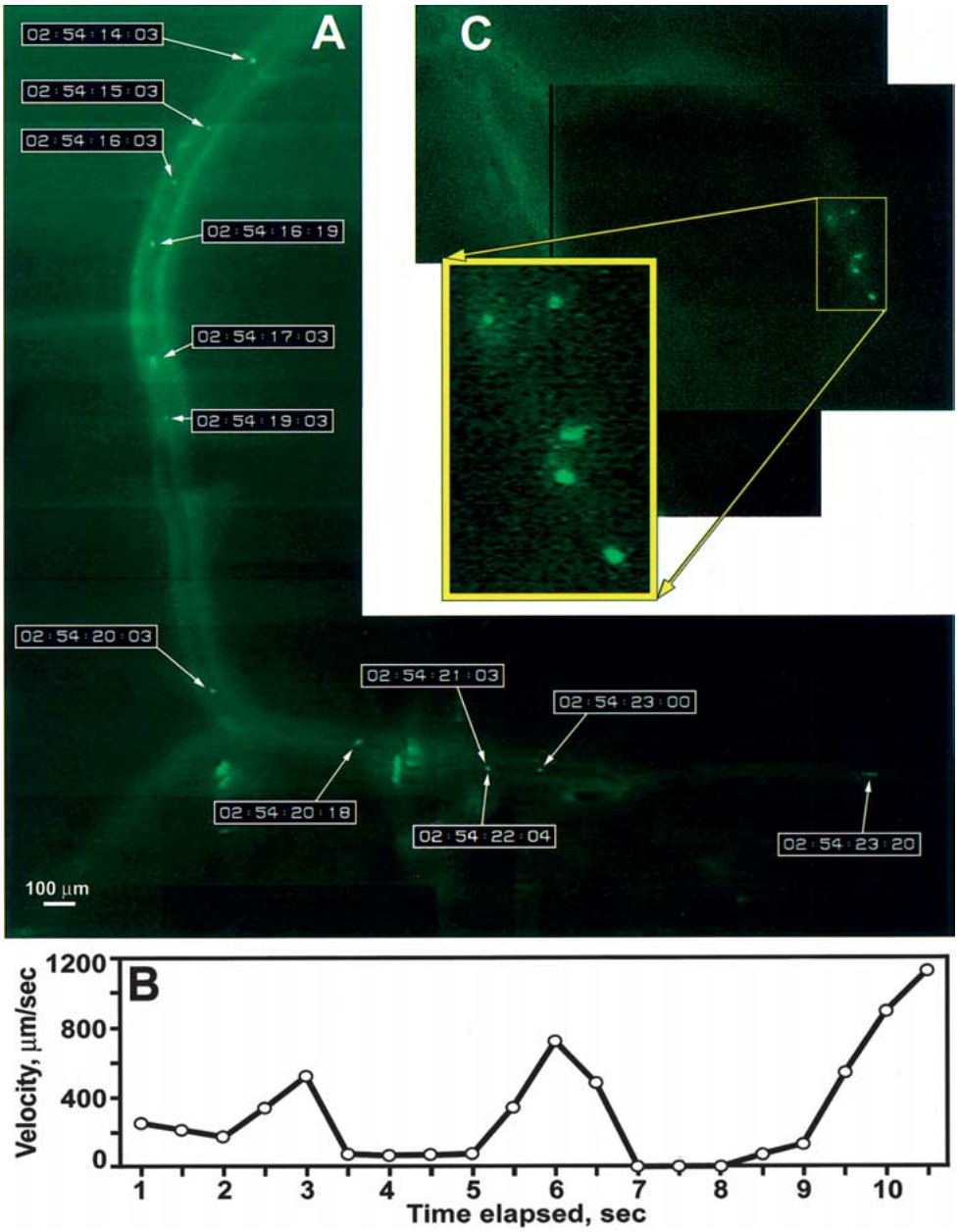

Figure 4. A, composite picture of 12 consequent frames illustrating the movement of the interacting/rolling prostate cancer cell (arrows) along perfused porcine dura mater microvasculature over 10.5 s period. Numbers in boxes show time code generator reading corresponding to each frame in hours, minutes, seconds, and frame numbers (30 frames/s) presented as hh:mm:ss:ff. B, the dynamics of the velocity changes of rolling prostate cancer cell shown in A over 10.5 s period. C, 'hot spot' within a pre-capillary arteriole harboring multiple cancer cells. Scale bar: 100 μm.

2–4-fold more adhesive to microvascular endothelium than their low metastatic counterparts [19]. These observations imply that, even though circulating malignant cells could roll on microvascular endothelium, rolling is not a prerequisite for their permanent adhesion to the vascular wall.

Importantly, we observed the vast majority of neoplastic cell adhesive interactions in pre capillary arterioles and capillaries. In contrast, leukocytes adhere to the endothelium and escape microcirculation in post capillary venules. Although, we cannot completely rule out tumor cell interactions with venular endothelium, this is an important observation suggesting that intravascular adhesion of tumor cells and leukocytes could be governed by adhesion molecules differentially expressed on different microvessels. In addition, even within arterial part of microcirculation, tumor cells adhesive interactions with endothelium of different microvessels or different segments of the same vessel varied significantly. For example, when individual cancer cell where followed along the vasculature, those that interacted with endothelium moved in a specific manner characterized by multiple discrete interruptions and rapid changes in velocity ranging from 0 to 2000 μm/s, (Figures 4A and B). In many instances, we observed multiple stably adhered tumor cells located within relatively short segments of pre capillary arterioles (Figure 4C), while the rest of the vessel as well as neighboring microvessels remained free of neoplastic cells. This observation suggests the existence of 'hot spots' within a microcirculation of metastasis prone organs, exhibiting

elevated ability to harbor metastatic cells compared to the rest of the microvasculature. Uncovering the factors defining this ability could be of paramount importance for our understanding of the molecular and cellular mechanisms underpinning hematogenous cancer spread.

The technology described herein provides investigators with great flexibility for studying metastatic cancer cell interactions with the microvasculature of a target organ. Most importantly, tumor cell adhesion could be studied in real time using intact microvessels in their native state in the context of the original tissue microenvironment, which warrants the persistence of the genuine adhesion molecules expression profiles. Moreover, cancer cells interacting with endothelia could be followed along the perfused vascular tree, and distinct steps of the adhesion process could be monitored continuously and video recorded over extended periods of time. This in turn, using selective inhibitors directed against various adhesion molecules expressed on endothelial and cancer cells, would allow for delineating the specific functions of different adhesion molecules at distinct stages of the metastatic process. Most importantly, these techniques produce consistent reproducible results, as we persistently observed prostate cancer cell adhesion patterns described herein in preparations from 15 animals.

While porcine dura mater was used in this study, this technique could be adapted easily for the study of metastatic tumor cell interactions with a variety of other porcine and human soft tissues frequently involved in cancer metastasis. The use of this technique will facilitate the uncovering of the molecular and cellular mechanisms of tumor metastasis.

Acknowledgements

This work was supported by National Institutes of Health P20 CA86290-01 (V.V.G.); P50 CA69568 (K.J.P.); R37 HL-42528-13 and PO1 HL52490-06 (V.H.H.); RO1 HL-36088-16 (J.R.T.); and T32 HL07094 (O.V.G.).

References

1. Al-Mehdi AB, Tozawa K, Fisher AB et al. Intravascular origin of metastasis from the proliferation of endothelium-attached tumor cells: A new model for metastasis. Nat Med 2000; 6: 100–2.
2. Orr FW, Wang HH, Lafrenie RM et al. Interactions between cancer cells and endothelium in metastasis. J Pathol 2000; 190: 310–29.
3. Padera TP, Stoll BR, So PTC et al. Conventional and high-speed intravital multiphoton laser scanning microscopy of microvasculature, lymphatics, and leukocyte-endothelial interactions. Mol Imaging 2002; 1: 9–15.
4. Cooper CR, Pienta KJ. Cell adhesion and chemotaxis in prostate cancer metastasis to bone: a minireview. Prost Cancer Prost Dis 2000; 3: 6–12.
5. Glinsky VV, Glinsky GV, Rittenhouse-Olsen K et al. The role of Thomsen-Friedenreich antigen in adhesion of human breast and prostate cancer cells to the endothelium. Cancer Res 2001; 61: 4851–7.
6. Glinsky VV, Huflejt ME, Glinsky GV et al. Effects of Thomsen-Friedenreich antigen-specific peptide P-30 on β-galactoside-mediated homotypic aggregation and adhesion to the endothelium of MDA-MB-435 human breast carcinoma cells. Cancer Res 2000; 60: 2584–8.
7. Lehr JE, Pienta KJ. Preferential adhesion of prostate cancer cells to a human bone marrow endothelial cell line. J Natl Cancer Inst 1998; 90: 118–23.
8. Scott LJ, Clarke NW, George NJR et al. Interactions of human prostatic epithelial cells with bone marrow endothelium: binding and invasion. Br J Cancer 2001; 84: 1417–23.
9. Nemeth JA, Harb JF, Barroso U et al. Severe combined immunodeficient-hu model of human prostate cancer metastasis to human bone. Cancer Res 1999; 59: 1987–93.
10. Yonou H, Yokose T, Kamijo T et al. Establishment of a novel species- and tissue-specific model of human prostate cancer in humanized non-obese diabetic/severe combined immunodeficient mice engrafted with human adult lung and bone. Cancer Res 2001; 61: 2177–82.
11. Rumbaut RE, Huxley VH. Similar permeability responses to nitric oxide synthase inhibitors of venules from three animal species. Microvascular Res 2002; 64: 21–31.
12. Rubin MA, Pitzi M, Mucci N et al. Rapid ('warm') autopsy study for procurement of metastatic prostate cancer. Clin Cancer Res 2000; 6: 1038–45.
13. Lehr H-A, Leunig M, Menger MD et al. Dorsal skinfold chamber technique for intravital microscopy in nude mice. Am J Pathol 1993; 143: 1055–62.
14. Rumbaut RE, Harris NR, Sial AJ et al. Leakage responses to L-NAME differ with fluorescent dye used to label albumin. Am J Physiol 1999; 276: H333–9.
15. Glinsky GV, Glinsky VV. Apoptosis and metastasis: A superior resistance of metastatic cancer cells to programmed cell death. Cancer Lett 1996; 101: 43–51.
16. Segre G, Silberberg A. Behavior of microscopic rigid particles in Poiseuille flow. II. Experimental results and interpretation. J Fluid Mech 1962; 14: 136–57.
17. Lawrence MB, Springer TA. Leukocytes roll on selectin at physiologic flow rates: Distinction from and prerequisite for adhesion through integrins. Cell 1991; 65: 859–73.
18. Butcher EC. Leukocyte-endothelial cell recognition: Three (or more) steps to specificity and diversity. Cell 1991; 67: 1033–6.
19. Khaldoyanidi SK, Glinsky VV, Sikora L et al. MDA-MB-435 human breast carcinoma cell homo- and heterotypic adhesion under flow conditions is mediated in part by Thomsen-Friedenreich antigen-galectinn-3 interactions. J Biol Chem 2003; 278: 4127–34.